VOL. 11, NO. 19, OCTOBER 2016 ISSN 1819-6608
ARPN Journal of Engineering and Applied Sciences

www.arpnjournals.com

EFFECT OF JET LENGTH ON THE PERFORMANCE OF PELTON TURBINE: DISTANCE BETWEEN NOZZLE EXIT AND RUNNER

Vishal Gupta[1], Vishnu Prasad[2] and Ruchi Khare[2]
[1]Department of Energy, M.A.N.I.T., Bhopal, MP, India
[2]Department of Civil Engineering, M.A.N.I.T., Bhopal, MP, India
E-Mail: vishalgupta.manit@gmail.com

ABSTRACT

Pelton turbine is the most commonly used high head impulse turbine with low discharge. For obtaining highest power output from runner one of the most important parameter is quality of jet which strikes bucket tangentially. The quality of jet and its impact work depends on the distance between the nozzle exit and runner along with its angle of strike. In the present paper, the effect of distance between the nozzle outlet and the runner on performance of Pelton turbine is discussed with the help of numerical technique. It is found that that axial flow of water is more for least (100 mm) distance while the radially inward and outward flow is more for larger (150 mm) distance between nozzle and runner.

Keywords: pelton runner, nozzle outlet, multiphase flow, free surface flow.

1. INTRODUCTION

Water is available at high head in hilly areas, so power generation using impulse turbine is common in hilly areas. Pelton is most commonly used impulse turbine used for high heads. Water after getting discharged from nozzle strikes in the form of compact jet tangentially to runner such that it is most of the time perpendicular to striking bucket. When water leaves from the nozzle, the cross-section of jet reduces to least diameter and then again it starts increasing. Least diameter of jet is found to be around at half the distance of nozzle diameter and that is called vena contracta. As the distance of jet increases, jet again starts to diverge. The cross-sectional area of jet when it strikes bucket affects overall performance of runner, water distribution on buckets, direction of flow. In present paper numerical simulation of a Pelton turbine is done by commercially available CFD code to study the effect of distance between nozzle outlet and runner on flow parameters.

2. LITERATURE REVIEW

Catanase *et al*. [1] numerically investigated jet from a Pelton turbine nozzle. They concluded that position of needle influence velocity distribution in the jet. The contraction diameter of the jet and its position are also determined. Matthias [2] *et al* has numerically simulated and validated impact of free jet on plate kept at various angles. Similar conditions were also applied to rotating flat plate runner. Experimental measurement of velocity of water coming out of various shapes of nozzles was done by Kotousov [3]. Perrig *et al*. [4], numerically and experimentally analysed flow pattern, pressure distribution in Pelton turbine bucket. Konnur *et al*. [5] have numerically analysed flow distribution of flat plate kept at various angles and applied to Pelton bucket. Experimental investigation of flow disturbances which affect the shape, orientation, and the topology of the jets leading to shift of the jet core from the axis of the nozzle was done by Zhang and Casey [6] using laser Doppler anemometry. Peron *etal*., [7] have numerically and experimentally discussed the importance of jet quality on Pelton turbine using two rehabilitation projects. Santolin *et al.*[8] numerically studied the jet interaction process and compared the results experimentally. Kubota [9] experienced jet interference in the model of 6 jet Pelton turbine model. Fiereder et al [10] numerically and experimentally investigated flow in Pelton turbine. Guha [11] numerically simulated high speed water jet in the air and validated it. Benzon et al. [12] have used CFX and Fluent for design optimisation for getting appropriate jet shape.

A lot of work has been done for jet shape and simulating water jet for Pelton runner. In present paper commercial software ANSYS CFX is used to study the effect of distance between the nozzle outlet and runner by varying the distance between them. Two cases i.e., 100 mm and 150 mm are simulated. Numerical results for 100 mm distance are validated against experimental available results from Pelton turbine model.

3. GOVERNING EQUATIONS

Fundamental governing equations of fluid dynamics i.e, the continuity, momentum and energy equations [13-14] which are in partial differential form are the base of CFD. These equations are based on conservation of mass momentum and energy.

Continuity Equation:

$$\frac{\partial \rho_m}{\partial t} + \vec{\nabla} \bullet \left(\rho_m \vec{W}_m\right) = 0$$

where the mixture density ρ_m and the mixture relative flow velocity $\vec{W}_m$ are defined as

$$\rho_m = \sum_{n=1}^{2} \alpha_n \rho_n \quad \text{and} \quad \bar{W}_m = \frac{\sum_{n=1}^{2} \alpha_n \rho_n \bar{W}_n}{\rho_m}$$

where the volume fraction α_n is given by

$$\alpha_n = \frac{V_n}{\sum_{n=1}^{2} V_n}$$

Momentum Equation:

$$\frac{\partial}{\partial t}\left(\rho_m \vec{W}_m\right)+\rho_m\left(\vec{W}_m \bullet \vec{\nabla}\right)\vec{W}_m = -\vec{\nabla}p_m + \vec{\nabla}\left(\bar{\bar{\tau}}_m + \bar{\bar{\tau}}_{t_m}\right) - \rho_m\vec{\omega}\times\left(\vec{\omega}\times\vec{r}_m\right) - 2\vec{\omega}\times\vec{W}_m + \vec{f}_m$$

4. FORMULAE USED

The theoretical power input is given by:

$$P_I = \rho \times g \times Q \times H \quad (1)$$

The actual output power is less than the above calculated value [1] due to friction. Numerically calculated power output is given by:

$$P_O = \frac{2 \times \pi \times N \times T}{60} \quad (2)$$

The hydraulic efficiency is given by:

$$\eta_h = \frac{P_o}{P_I} \quad (3)$$

Time step corresponding to 1° runner rotation was found out using:

$$\Delta t = \frac{60}{360 \times N} \quad (4)$$

Speed coefficient is given by:

$$\varphi_B = \frac{\pi \times N \times D}{60\sqrt{2 \times g \times H}} \quad (5)$$

Blade Loading Coefficient: Pressure variation along streamwise direction in dimensionless form is expressed as:

$$Cp = \frac{P}{\frac{1}{2}\rho C_1^2} \quad (6)$$

Absolute velocity coefficient:

$$K_c = \frac{C}{\sqrt{2 \times g \times H}} \quad (7)$$

Loss coefficient: It is the ratio of whirl velocity at outlet to inlet.

$$K_L = \frac{W_2}{W_1} \quad (8)$$

Discharge Coefficient: In non dimensional form it is expressed as:

$$K_Q = \frac{4 \times Q}{\pi \times B^2 \times Z \times \sqrt{2 \times g \times H}} \quad (9)$$

5. GEOMETRIC MODELING

The domain for analysis needs to be numerically simulated in 2-dimensional or 3-dimensional geometry depending upon requirement. For the present study, domain from the exit of nozzle to runner is generated. Only three symmetrical half jets with 10 symmetrical half buckets (half of the rotor) were modeled due to limitation of computational power. The complete flow domain consists of stator containing water jet and rotating domain containing buckets. The modeling has been done by using commercial software. The modeled geometry of domain containing water jet (both short distance and long distance between nozzle exit and runner) and Pelton turbine has been shown in Figure-1, Figure-2 and Figure-3, respectively.

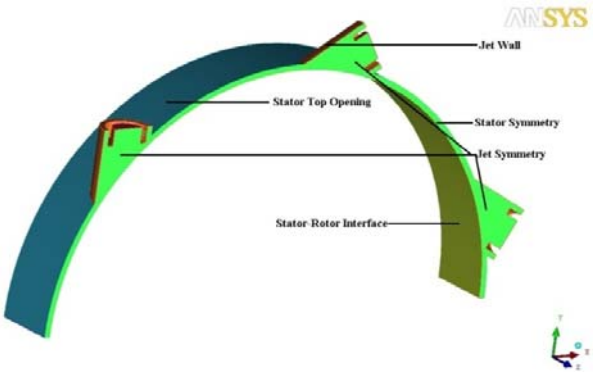

Figure-1. Geometry of stator domain with 100 mm distance.

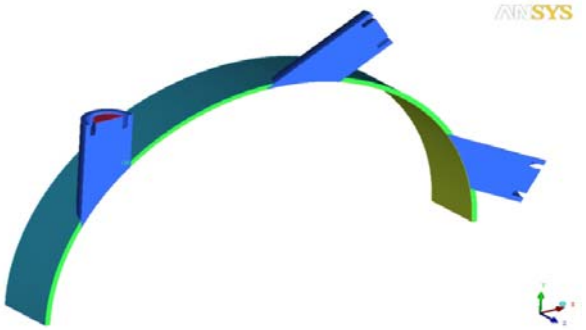

Figure-2. Geometry of stator domain with 150 mm distance.

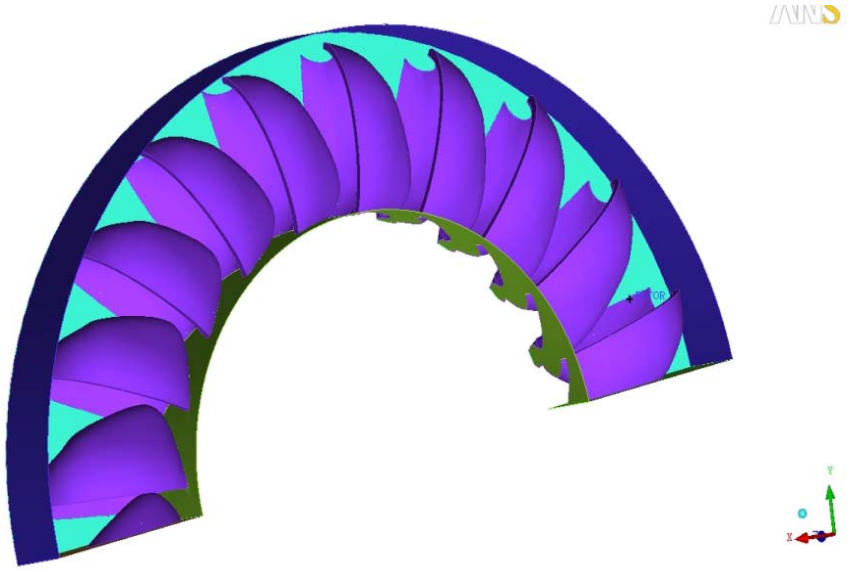

Figure-3. Geometry of rotor domain.

6. MESH GENERATION

The complete domain for analysis needs to discretised into small elements which are known as mesh. The mesh has tetrahedral and prismatic 3-D elements for volume and triangular elements at the surface. Prism layer has been applied to jet wall and bucket surface to capture the flow accurately.

Table-1. Mesh data for short distance between nozzle exit and runner (100 mm).

Part name	No. of nodes	No. of elements	Element type
Jet inlet	1248	1469 399	Triangular Quadrilateral
Jet wall	16147	31348	Triangular
Jet symmetry	6636	9851 1305	Triangular Quadrilateral
Stator top opening	36340	71087	Triangular
Stator side opening	3293	5263	Triangular
Stator symmetry	2497	4024	Triangular
Periodic surface 1	262	416	Triangular
Periodic surface 2	255	402	Triangular
Stator rotor interface	39564	77712	Triangular
Flow space	456213	2146945 1089	Tetrahedral Pyramids

7. BOUNDARY CONDITIONS

The nozzle is fixed, so stator domain is kept stationary. Buckets rotate so domain containing buckets i.e., rotor domain has been set at speed corresponding to Best Efficiency Point (BEP) which is 820 rpm. SST turbulence model is taken for analysis because of its capability to capture sharp curvatures and complexities in the flow.

Transient flow simulation with time step corresponding to l° runner rotation has been done. The working fluids are air and water with a reference pressure of 1 atmosphere. The jet inlet has been defined as inlet with water velocity corresponding to 50 m head. Jet symmetry, stator symmetry and rotor symmetry have been defined as symmetry and periodicity has been applied at both symmetric ends of the stator and rotor. Opening is specified at stator side opening, stator top opening, rotor side opening and rotor mid opening with a relative pressure of 0 atmospheres. Suitable interfacing is applied between stator and rotor domains.

8. RESULTS AND DISCUSSIONS

8.1 Validation

Efficiency obtained for shorter distance between nozzle exit and runner is compared with the efficiency of available model test result. Experimental efficiency is 90.5% at rated speed and discharge whereas numerical efficiency is found out to be 88.03% which is in very close agreement.

8.2 Variation in torque experienced by runner

The torque experienced by rotor for 100 mm and 150 mm distance is plotted in Figure-4.

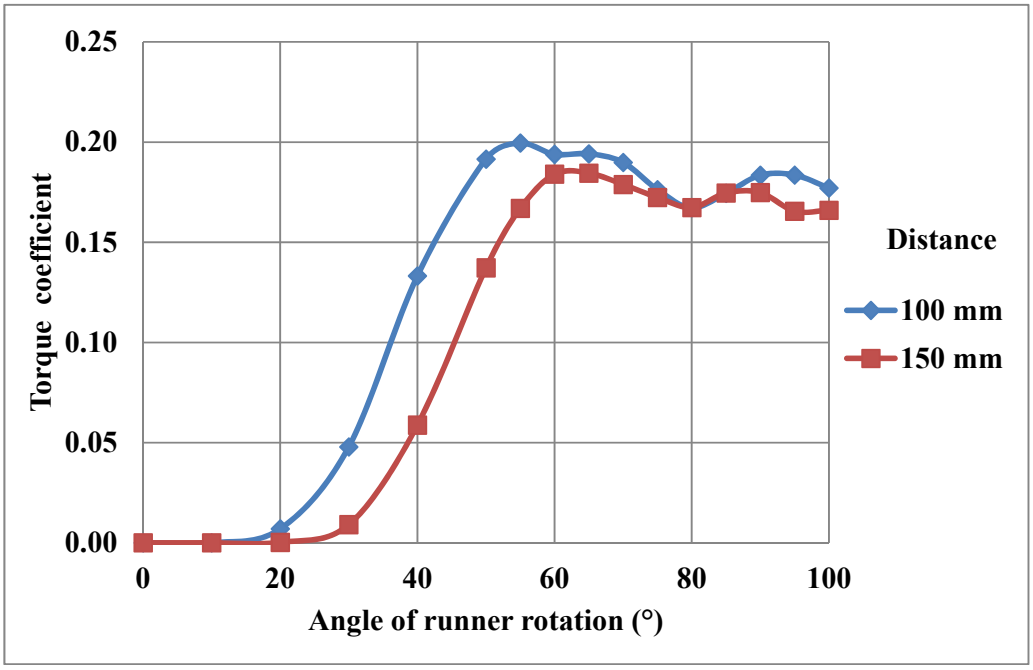

Figure-4. Variation in torque experienced by rotor for different distances between nozzle and bucket

It is observed from Figure-4 that variation in torque experienced by rotor with change in bucket angular position is of similar type for both jets. The jet strikes the runner earlier in case of 100 mm distance as compared to 150 mm distance so increase in torque with bucket angular position is observed for 100 mm distance. The torque experienced by rotor is more for 100 mm distance than 150 mm distance nearly at all angular positions of bucket.

8.3 Streamwise blade loading

The blade loading pattern in Figure-5 indicates that pressure rise at inlet and blade loading is more for 100 mm distance.

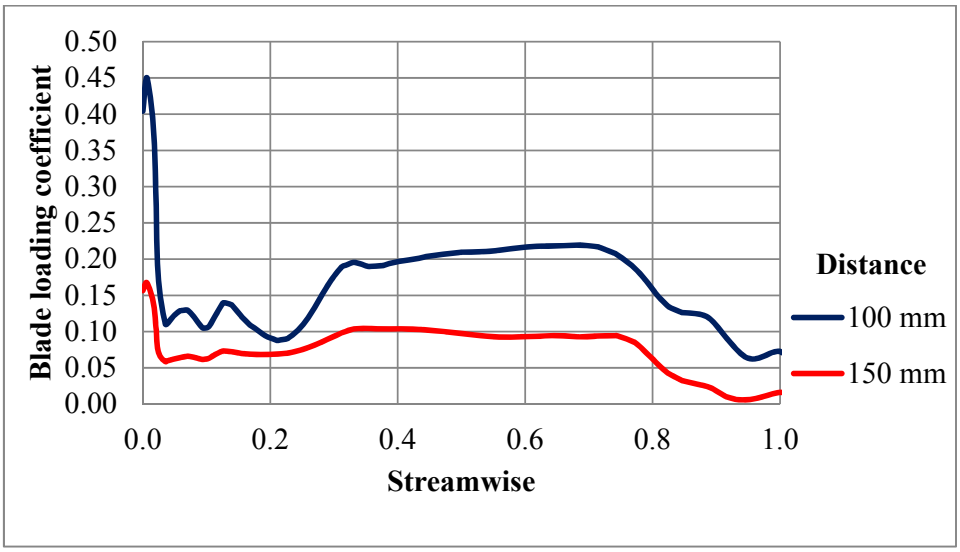

Figure-5. Variation in blade loading at mid span for different distances between nozzle and bucket.

8.4 Streamwise variation in absolute velocity

The streamwise variation of absolute velocity from inlet to outlet in Figure-6 shows gradual decrease of velocity from splitter to outlet for both distances. The absolute velocity at outlet is nearly same while at inlet it is found to be more for 100 mm distance. This is because on increasing the distance from nozzle exit to runner, water jet discharging from nozzle spreads and gives lessr impact to the runner.

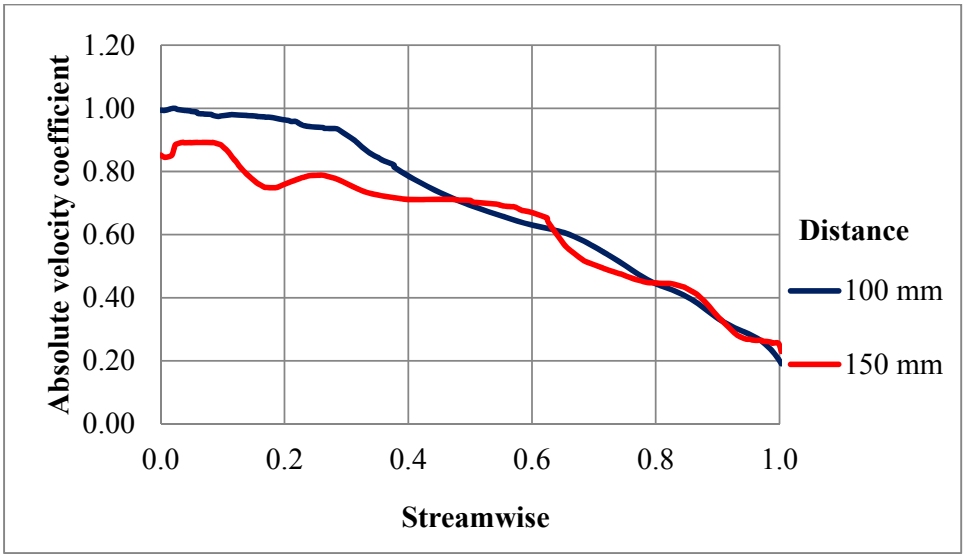

Figure-6. Variation in absolute velocity coefficient at mid span for different distances between nozzle and bucket.

8.5 Flow distribution

The water volume fraction iso surface for both the cases (i.e., 100 mm and 150 mm distance) are shown in Figure-7 and Figure-8 respectively. In case of 100 mm distance, buckets do not get emptied fully before reaching in front of next jet rather a part of water sheet near to exit of bucket can be seen. But in case of 150 mm distance, the buckets get fully emptied before reaching next jet.

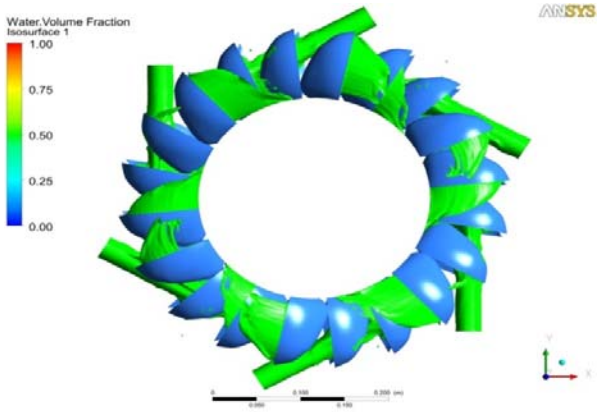

Figure-7. Flow distribution for 100 mm distance at BEP.

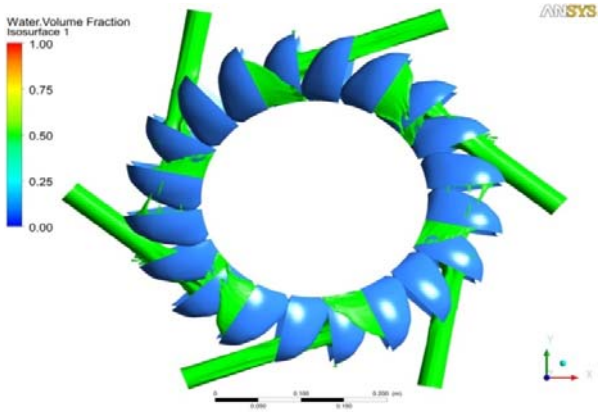

Figure-8. Flow distribution for 150 mm distance at BEP.

The water volume fraction for 100 mm and 150 mm distance at 0.25, 0.5 and 0.75 span are shown in Figure-9.

At 0.25 span, some buckets are seen fully empty for 100 mm distance and buckets in front of jet have water at mid stream length but in case of 150 mm distance no bucket is seen fully empty. The water is seen more at inlet for bucket in front of jet and less at outlet in other buckets at 0.5 span. As seen in Figure-9(c), water at inlet of bucket is observed only in the bucket which are in front of jet.

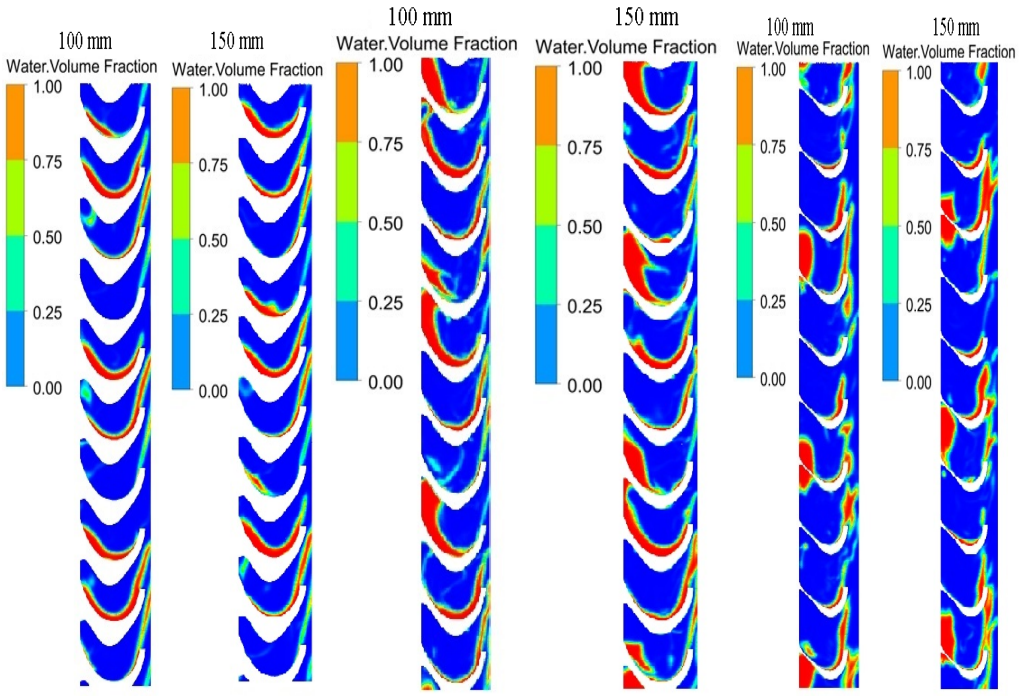

Figure-9. Variation in water volume fraction at 0.25, 0.50 and 0.75 span.

Table-2. Average values of velocity coefficients for different distance between nozzle exit and bucket.

	Distance between nozzle and bucket			
	100 mm		150 mm	
	Inlet	Outlet	Inlet	Outlet
Relative velocity coefficient	0.51	0.46	0.51	0.44
Absolute velocity coefficient	1.00	0.18	1.00	0.17
Whirl Velocity coefficient	1.00	0.06	1.00	0.07
Tangential velocity coefficient	0.49	0.49	0.49	0.49
Flow angle	0	21.10	0	19.88

Table-3. Average values of non-dimensional parameters for different distance between nozzle and bucket.

Distance	K_T	K_L	K_Q	ϕ_B	η
100 mm	0.185	0.899	0.077	0.48	88.03
150 mm	0.170	0.874	0.077	0.48	84.62

Table-4. Water distribution at exit of runner for different distance between nozzle and bucket.

Distance	Axial (%)	Radially inward (%)	Radially outward (%)
100 mm	89.93	9.09	0.98
150 mm	85.54	11.38	3.08

The relative and absolute velocity in Table-2 is found to be less and whirl velocity is more for 150 mm distance. The flow angle at outlet for 150 mm distance is less than that of 100 mm.

The torque, frictional loss and efficiency is found to be higher for 100 mm jet length as given in Table-3 because of lesser loss in case of 100 mm jet length.

It is seen from Table-4 that axial flow of water is more for 100 mm distance while the radially inward and outward flow is more for 150 mm distance.

9. CONCLUSIONS

It is found that the length of jet i.e., distance between nozzle exit and runner effects the performance of Pelton turbine. The torque experienced by runner is delayed for 150 mm distance and torque coefficient and efficiency is maximum for 100 mm distance. The blade loading is more for 100 mm distance.

The absolute velocity decreases from inlet to outlet. The average relative, absolute and whirl velocities at outlet are seen to be nearly independent of jet distance. The flow angle at outlet decreases as the distance increases.

The loss coefficient also decreases with increase in jet distance. The axial flow decrease and radial flow increase as the distance between jet and bucket is increased.

Notations used

B	bucket width (m)
C_1	absolute velocity at runner inlet (m/s)
C_p	pressure coefficient
D	runner diameter (m)
d_0	diameter of jet at outlet of nozzle (m)
d_1	diameter of jet at vena contracta (m)
g	acceleration due to gravity (m/s2)
H	net available heat at inlet of nozzle (m)
hf	total head loss (m)
k	friction factor
K_C	absolute velocity coefficient
K_L	loss coefficient
K_Q	discharge coefficient
K_T	torque coefficient
K_u	speed ratio
L	bucket length (m)
N	rotational speed of runner (rpm)
P	static pressure at any point (Pa)
P_I	power supplied from jet to runner
P_O	Power available at the nozzle inlet (Watt)
Q	Discharge (m3/sec)
T	torque available at runner (N-m)
U_1	absolute velocity of runner (m/s)
U_2	tangential velocity of runner at outlet (m/s)
Z	number of buckets
η_H	hydraulic efficiency
ρ	density of fluid (kg/m3)
φ_B	speed coefficient

REFERENCES

[1] Catanase A., Barglazan M. and Hora C. 2004. Numerical Simulation of a Free Jet in Pelton Turbine. Proceedings of 6th International Conference on Hydraulic Machinery and Hydrodynamics Timisoara. Romania. pp. 79-84.

[2] Matthias H.B. and Promper O. 2004. Numerical Simulation of the Free Surface Flow in Pelton Turbines. Proceedings of 6th International Conference

on Hydraulic Machinery and Hydrodynamics Timisoara. Romania. pp. 119-124.

[3] Kotousov L.S. 2005. Measurement of the Water Jet Velocity at the Outlet of Nozzles with Different Profiles. Transaction of Technical Physics. 50(9): 1112-1118.

[4] Perrig A., Avellan F., Kueny J.L. and Farhat M. 2006. Flow in a Pelton Turbine Bucket: Numerical and Experimental Investigations. Transaction of ASME. 128: 350- 358.

[5] Konnur M.S. and Patel K. 2006. Numerical Analysis of Water Jet on Flat Plate. Proceedings of National Conference on Fluid Mechanics and Fluid Power. Raipur. India.

[6] Zhang Z. and Casey M. 2007. Experimental Studies of the Jet of a Pelton Turbine. Journal of Power and Energy. 221(Part A): 1181-1192.

[7] Peron M., Parkinson E., Geppert L. and Staubli T. 2008. Importance of Jet Quality on Pelton Efficiency and Cavitation. Proceedings of 7th International Conference on Hydraulic Efficiency Measurements. IGHEM 2008. Milan. Italy.

[8] Santolin A., Cavazzini G., Ardizzon G. and Pavesi G. 2009. Numerical Investigation of the Interaction between the Jet and Bucket in a Pelton Turbine. Journal of Power and Energy. 223(Part A): 721-728.

[9] Kubota T. 2010. Observation of Jet Interference in 6-Nozzle Pelton Turbine. Journal of Hydraulic Research. 27(6): 753-767.

[10] Fiereder R., Riemann S. and Schilling R. 2010. Numerical and Experimental Investigation of the 3D Free Surface Flow in a Model Pelton Turbine. Proceeding of 25th IAHR symposium on Hydraulic Machinery and Systems. Timisoara. Romania.

[11] Guha A., Barron R.M. and Balachandar R. 2010. Numerical Simulation of High Speed Turbulent Water Jets in Air. Journal of Hydraulic Research. 28(1): 119-124.

[12] Benzon D., Židonis A. Panagiotopoulos A.,Aggidis G.A.,Anagnostopoulos J.S. and PapantonisD.E. 2015. Numerical Investigation of the Spear Valve Configuration on the Performance of Pelton and Turgo Turbine Injectors and Runners. Journal of Fluids Engineering. 137(11): Article ID 111201.

[13] Anderson John D. 1995. Computational Fluid Dynamics, McGraw-Hill Inc. New York.

[14] ANSYS CFX user manuals. Ansys Inc. USA.